ADSORPTION OF COPPER (II) IONS IN WASTEWATER USING MANGROVE-BASED ACTIVATED CARBON

MUHAMMAD HAKIMI FIRDAUS BIN MAMAT

UNIVERSITI SAINS MALAYSIA

2022

ADSORPTION OF COPPER (II) IONS IN WASTEWATER USING MANGROVE-BASED ACTIVATED CARBON

by

MUHAMMAD HAKIMI FIRDAUS BIN MAMAT

Project report submitted in partial fulfilment of the requirement for the degree of Bachelor of Chemical Engineering with Honours

2022

ACKNOWLEDGEMENTS

This final year project is for the completion of degree of Bachelor of Chemical Engineering. Firstly, I would like to express my gratitude to Allah S.W.T for granting me the strength in completing this report for this thesis. Other than that, I would like to show my highest gratitude and appreciation to all the individuals involved for their contribution throughout the project.

I would also like to express my sincere appreciation to my supervisor, Associate Professor Dr. Ridzuan Zakaria for his irreplaceable supervision, understanding direction and endless inspiration throughout this project. Without the supervision and advice from him, this final year project will not be done entirely on time. Also, I would like to express my deepest gratitude to Professor Mohd Azmier's, post-doctoral researcher, Dr. Firdaus that also guided me throughout this project.

Once again, I would like to thank all the people, including those who I might have missed out on mentioning their names but have helped me directly or indirectly in the accomplishment of this project. Thank you very much.

Muhammad Hakimi Firdaus Bin Mamat

June 2022

TABLE OF CONTENTS

LIST OF TABLES

LIST OF FIGURES

LIST OF SYMBOLS

Symbol	Description	Unit
$1/n$	Heterogeneity factor	-
C_1	Concentration of stock solution	M or ppm
C_2	Final concentration after dilution	M or ppm
C_e	Equilibrium metal ion concentration after adsorption	ppm or mg/L
C_o	Initial metal ion concentration	ppm or mg/L
K	Langmuir equilibrium coefficient	L/mg
K_e	Adsorption equilibrium constant	L/g
K_F	Freundlich constant	L/mg
k_1	Rate constant of PFO kinetic	min^{-1}
k_2	Rate constant for PSO adsorption kinetic	g/mg. min
M	Amount of adsorbent	g
q_e	Amount of metal ion uptake/Adsorption equilibrium	mg/g
q_{max}	Maximum adsorption capacity	mg/g
q_t	Adsorption capacity taken at time	$mg/g_{adsorbent}$
R	Gas constant	J/mol. K
T	Absolute temperature	K
t	Time taken to reach equilibrium	min
V_1	Volume of stock solution reuqired	mL or L
V_2	Final volume of diluted solution	mL or L
W	Watt (unit of power)	-
ΔG^o	Standard Gibbs free energy	J/mol
ΔH^o	Standard enthalpy	J/mol
ΔS^o	Standard entropy	J/mol

LIST OF ABBREVIATION

Symbol	Description
AAS	Atomic Absorption Spectrometer
AC	Activated Carbon
BET	Brunauer–Emmett–Teller
CCD	Central Composite Design
CHNS	Carbon Hydrogen Nitrogen Sulphur
FTIR	Fourier Transform Infrared
IR	Impregnation Ratio
IUPAC	International Union for Pure and Applied Chemistry
MW	Molecular Weight
PFO	Pseudo-First-Order
PSO	Pseudo-Second-Order
R^2	Correlation Coefficient
RSM	Response Surface Methodology
SEM	Scanning Electron Microscope
Δq	Normalized Standard Deviation of Adsorption Capacity

PENJERAPAN ION KUPRUM (II) DARI AIR SISA DENGAN KARBON TERAKTIF DARIPADA BATANG BAKAU

ABSTRAK

Pencemaran air telah menjadi masalah yang teruk akibat daripada pembuangan air sisa industri yang mengandungi logam berat. Matlamat utama penyelidikan adalah untuk menambah baik keadaan penyediaan dan penjerapan karbon teraktif yang diperbuat daripada bahan mentah kos rendah. Pengaktifan pemanasan gelombang mikro karbon teraktif berasaskan bakau adalah kos efektif memandangkan hutan bakau banyak terdapat di Malaysia, dan pemanasan gelombang mikro mengambil sedikit masa dan menggunakan lebih sedikit tenaga elektrik. Pada 616 W dan 2 minit di bawah aliran nitrogen, karbon teraktif terbaik dihasilkan. Dengan 99.67 peratus hasil karbon teraktif dan 77.256 peratus penyingkiran ion kuprum (II), nisbah KOH: Char yang optimum didapati berada pada IR 0.75. Spektroskopi inframerah transformasi Fourier, isoterma penjerapan/penyahsorpsi nitrogen, dan analisis unsur digunakan untuk menganalisis AC. Selain daripada pengoptimuman, proses penjerapan menggunakan penjerap bakau telah disiasat dalam situasi yang berbeza. Penjerapan mencapai keseimbangan selepas 3 jam pada 10ppm dan 60°C, menurut data eksperimen. Sifat penjerapan berbilang lapisan dan heterogen dijelaskan oleh model isoterma Freundlich dengan nilai R2 0.9995 dan 1/n kurang daripada satu. Kapasiti penjerapan maksimum karbon teraktif berasaskan bakau yang diukur menggunakan Isoterma Langmuir ialah 33.557 mg/g, menunjukkan janjinya sebagai penjerap. Tambahan pula, dengan nilai R2 0.9997, data telah berjaya dipasang pada model kinetik tertib pseudo kedua. Akhir sekali, analisis termodinamik mendedahkan bahawa penjerapan yang disiasat adalah proses endotermik, dengan penjerapan spontan pada 50 dan 60 darjah Celsius.

ADSORPTION OF COPPER (II) IONS IN WASTEWATER USING MANGROVE-BASED ACTIVATED CARBON

ABSTRACT

Water contamination has become a severe problem as a result of the discharge of industrial wastewater containing heavy metals. To support the pollutant adsorption approach, a low-cost adsorbent is necessary. The research's major goal is to improve the preparation and adsorption conditions of activated carbon made from low-cost raw materials. Microwave heating activation of mangrove-based activated carbon is cost-effective since mangrove is abundant in Malaysia, and microwave heating takes less time and uses less electricity. At 616 W and 2 minutes under nitrogen flow, the best activated carbon was produced. With 99.67 percent activated carbon yield and 77.256 percent copper (II) ions elimination, the optimal KOH: Char ratio was found to be at an IR of 0.75. Fourier transform infrared spectroscopy, nitrogen adsorption/desorption isotherm, and elemental analysis were used to analyze the AC. Apart from optimization, the adsorption process employing the mangrove adsorbent was investigated under different situations. The adsorption reached equilibrium after 3 hours at 10ppm and 60°C, according to the experimental data. The multilayer and heterogeneous nature of adsorption is explained by Freundlich isotherm models with R2 values of 0.9995 and 1/n less than one. The maximum adsorption capacity of mangrove-based activated carbon measured using the Langmuir Isotherm was 33.557 mg/g, demonstrating its promise as an adsorbent. Furthermore, with an R2 value of 0.9997, the data was successfully fitted to pseudo-second-order kinetics models. Finally, the thermodynamic analysis revealed that the adsorption investigated is an endothermic process, with spontaneous adsorption at 50 and 60 degrees Celsius.

CHAPTER 1

INTRODUCTION

Chapter 1 provides an overview of this study and summarizes the heavy metal research background, the problem description, the project's purpose, and the project's outline.

1.1 Background

Copper (Cu), Chromium (Cr), Cadmium (Cd), Iron (Fe), Lead (Pb), Nickel (Ni), Zinc (Zn), and Arsenic (As) are the most common heavy metals found in the industry (As). These heavy metals are employed in the manufacture of textile dye pigments (Bhardwaj, Kumar and Singhal, 2014). Copper (II) ions were discovered in concentrations ranging from 0.17 to 0.28 mg/L. Copper (Cu), Manganese (Mn), Chromium (Cr), Iron (Fe), Cadmium (Ca), Nickel (Ni), and Lead (Pb) are also detected in wastewater from pulp and paper mills (Mandeep et al., 2019).

Furthermore, Buhari and Ismai (2020) describe the substantial heavy metal pollution (Cu, Zn, Pb, Cd, and Ni) in the surface sediments of Malaysia's west coast. Kuala Juru, Sungai Puluh, Bagan Lalang, Minyak Beku, and Sungai Tiga were among the sampling sites investigated. Jetty, industrial, and agricultural areas were all used as sampling locations. More than 700 organic and inorganic contaminants were identified in the watercourses of the sampling sites, according to reports. Heavy metal ions are the most harmful of these contaminants because of their poisonous and carcinogenic qualities. Some heavy metal ions are also non-biodegradable and non-transformable (Ali, 2010).

Copper is a heavy metal contaminant that is commonly found in water. It's a vital cofactor for enzymes that's always available for human growth and development.

Copper in a compound form, such as copper sulphate, is toxic to the human respiratory system, causing gastrointestinal anemia, numerous capillary damage, liver disease, and kidney malfunction (Ugwu and Agunwamba, 2020). Wastewater from agricultural fields and industrial regions such as electrical, metal finishing, paint, electroplating, pigment, and wood making industries are the main sources of contamination (Ali, 2012).

1.2 Problem Statement

The maximum concentration of copper ions discharged for standard A is 0.2 mg/L and 1.0 mg/L for standard B, according to the Environmental Quality Act 1974: Environmental Quality (Sewage And Industrial Effluents) Regulations 1979, where standard A is used when the discharge point is upstream of a water intake point for consumption or water catchment areas, and standard B is used when the discharge point is into the water catchment area (Malaysia Government, 1979). As a result, copper must be removed from wastewater before it may be dumped into any water source.

To remove copper (II) ions from wastewater, many water purification technologies are available, including reverse osmosis, ion exchange, electrodialysis, electrolysis, filtration, adsorption, and centrifugation. Except for adsorption, the cost of these present methods ranges from USD 10 to USD 450 (RM 40.41 to RM 1818.22) per cubic metre of water. The cost of activated carbon adsorption, on the other hand, ranges from 5 to 200 USD (RM 20.20 to RM 808.10) per cubic metre of water (Ali, 2010).

However, a large amount of adsorbent is necessary to remove the heavy metal from a large volume of wastewater, resulting in a hefty financial outlay. Because of its small particle sizes and active free valences, activated carbon is an effective adsorbent for heavy metal adsorption. Furthermore, adsorption using activated carbon appears to be the most frequent approach, owing to its ease of preparation and renewal. As a result, finding a low-cost alternative source material and heating technique to synthesis activated carbon is critical. The mangrove stem was chosen as the low-cost raw material for this project, while microwave heating was chosen as the less expensive heating technology. The properties and adsorption performance of the activated carbon that was formed were also investigated.

1.3 Objectives

The research work in this thesis is performed to achieve the objectives as listed below:

i. To investigate the factors that affect the characteristics of mangrove-based activated carbon.
ii. To study the factors that affect the copper (II) ions adsorption efficiency onto mangrove-based activated carbon.
iii. To determine the adsorption isotherm of copper (II) ions adsorption using mangrove-based activated carbon.
iv. To investigate the adsorption kinetics of copper (II) ions adsorption using mangrove-based activated carbon.

1.4 Thesis Outline

This thesis is divided into five sections. The contents of each chapter in this research are as follows: The problem statements, the objective, and the outline of this thesis are briefly introduced in Chapter 1 Introduction, which summarizes the study background of heavy metal, as well as the problem statements, the objective, and the outline of this thesis. The prior investigations and reviews available from scientists and researchers relevant to this topic are presented in Chapter 2 Literature review. The synthesis of activated carbon, the adsorption isotherm, adsorption kinetics, and adsorption performance are all covered in this chapter. The chapter discusses the factors that determine the pore distribution and adsorption capacity of activated carbon. The main research flow diagram, methodology specifics on activated carbon optimization, materials, equipment, and a copper (II) ions adsorption experiment are all covered in Chapter 3 Methodology. In addition, the results of mangrove-based activated carbon optimization and copper (II) ion adsorption tests are covered in Chapter 4 Results and Discussion. Based on the experimental results, ideal activated carbon fabrication and adsorption conditions are suggested and discussed. Finally, Chapter 5 concludes with a summary of the experiment findings as well as recommendations for future researchers.

CHAPTER 2

LITERATURE REVIEW

The past discoveries and reviews available from reputable scientific sources and references linked to this topic are presented in Chapter 2. This chapter also discusses the synthesis of activated carbon and its adsorption performance.

2.1 Removal of Copper (II) Ions by Adsorption Method

Adsorption with activated carbon is a surface phenomenon in which contaminants are adsorbed on the activated carbon's solid surface. Adsorbate refers to contaminants that cling to a solid surface, while adsorbent refers to the solid surface itself. The nature of the adsorbate and adsorbent, as well as the presence of other contaminants and experimental variables such as contact time, pH and concentration of adsorbate solution, temperature of solution, and adsorbent dosage, all influence adsorption. Isotherm models are often used to describe the adsorption mechanism, and the kinetics model is used to establish the limiting rate. By varying the temperature of the adsorbate solution, the thermodynamic parameters of the adsorption process are also investigated.

Different carbon sources have been used to manufacture activated carbon for copper (II) ions adsorption in industrial wastewater treatment in recent studies. Table 2.1 shows various activated carbons made from various source materials and activation processes for the adsorption of Cu (II) ions. Their maximal adsorption capacities (mg/g) on Cu (II) ions from their best-fit isotherm model are also included in the table based on their properties and ideal operating circumstances as determined by the researchers. Chemical activation was carried out using microwave and traditional heating procedures. Under nitrogen flow, the traditional heating process was carried out in a furnace at various temperatures (about 400-600°C) for more than

30 minutes. While microwave heating was done in a microwave oven with a microwave activation power and time based on the microwave's capability of less than 30 minutes.

Both biomass and wood-based activated carbon can be made using either traditional or microwave heating, as shown in Table 2.1. The greatest Qmax obtained using conventional heating technique was 90.90mg/g using modified cassava tuber bark (wood based), whereas the highest Qmax obtained using microwave heating technique was 33.56mg/g utilising modified mangrove stem in the current project. Furthermore, when the Qmax of microwave-heated and conventionally heated modified olive stone was compared, it was discovered that microwave-heated olive stone (22.73mg/g) had a higher Qmax than conventionally heated olive stone (17.83mg/g) (Alslaibi et al., 2014).

2.2 Preparation of Activated Carbon

Carbonization at high temperatures in an inert atmosphere is frequently followed by the activation procedure to generate activated carbon. The activation step has a considerable impact on the characterization of the activated carbon generated, resulting in varied adsorption performance. During the activation process, a porous surface is frequently generated. Physical and chemical activation are the two types of activation processes. The physical activation procedure required heating char obtained from carbonization and treating it with oxidizing gases like steam or carbon dioxide. Because the pores generated during carbonization are filled with pyrolysis residues, activation is required to expand the activated carbon's internal surface (Hidayu and Muda, 2016).

Table 2.1 Comparison of activation technique and maximum adsorption capacity of activated carbon derived from different carbon sources (biomass and wood-based).

Activation technique	**Source**	**Max. adsorption capacity, Q_{max} (mg/g)**	**Ref.**
Conventional	Chitosan	43.47	(Kannamba *et al*., 2010)
	Lentil shell	9.59	(Aydin *et al.*, 2008)
	Rice shell	2.95	
	Wheat shell	17.42	
	Black carrot	8.88	(Güzel, Yakut and Topal, 2008)
	Soybean straw	48.14	(Zhu, Fan and Zhang, 2008)
	Agaricus bisporus	11.44	(Ertugay and Bayhan, 2010)
	Ceiba pentandra hulls	20.80	(Madhava Rao *et al.*, 2006)
	Modified olive stone	17.83	(Alslaibi *et al.*, 2014)
	Sugarcane bagasse	0.45	(Salihi, Kutty and Ismail, 2018)
	Corn straw	12.52	(Chen *et al.*, 2011)
	Hardwood	6.79	
	Modified cassava tuber bark	90.90	(Horsfall, Abia and Spiff, 2006)
	Modified oakwood sawdust	3.22	(Argun *et al.*, 2007)
	Modified mangrove Barks (*Rizophora apiculate)*	5.80	(Rozaini *et al.*, 2010)
Microwave	Bagasse	25.12	(Wan and Li, 2018)
	Modified sewage sludge	10.56	(Wang *et al.*, 2011)
	Modified olive stone	22.73	(Alslaibi *et al.*, 2014)

An activation reagent such as ZnCl2, H3PO4, H2SO4, KOH, or NaOH is mixed with the raw material and heated in an inert atmosphere in the chemical activation process. To create varied pore sizes, different activating agents are utilised. Furthermore, the most essential elements that affect the final pore structure, surface area, and chemistry of the carbon produced are the temperature and time for activation.

Conventional heating is typically used for activation. Hesas et al. (2013) and Marda and Astuti (2017), on the other hand, reveal that conventional heating consumes a lot of energy, time, and money. According to both studies, during conventional heating, the heat source is positioned outside the carbon bed, and energy is transported to the sample by convection, conduction, and radiation from the inner surface to the interior. As a result, a temperature gradient exists between the hot activated carbon surface and the inside of the carbon. Because certain volatile components may remain in the activated carbon, this thermal gradient prevents the release of gaseous products such as pyrolysis gas into the atmosphere and leads to uniform heat distribution. To eliminate the temperature differential and obtain the target temperature, the heating rate is reduced and the activation period is longer. Heating for a longer period of time will almost certainly increase the cost and energy consumption.

Microwave heating, on the other hand, can be used for activation. Microwave heating takes place inside a microwave oven with a variable range of radiation strength and time, allowing inert gases such as nitrogen to flow into the raw materials to be activated. To improve the pore distribution in the activated carbon generated, an activating agent is still necessary for impregnation. Microwave heating has recently been offered as an alternative to traditional heating in the creation of activated carbon

for colour removal. Microwave heating, as opposed to traditional heating, produces activated carbon that performs better in adsorption in a shorter activation period, saving energy and money. According to Baytar, et al. (2018), Marda and Astuti (2017), and Alslaibi et al. (2014), microwave energy can be easily converted to heat and transferred inside the particles via dipole rotations and ionic conduction, resulting in a massive temperature gradient that steadily decreases from the sample's interior to its surface bulk. At a low bulk temperature, this temperature gradient permits the microwave-induced reaction to proceed more aggressively and effectively, triggering partial breakdown of volatile chemicals during the activation phase.

The comparison of activated carbon generated using traditional and microwave heating is shown in Table 2.2. Microwave heating requires a significantly shorter activation time than conventional heating, yet it nevertheless produces a comparable activated carbon with higher adsorption capacity, according to the comparison. Higher adsorption capacity suggests more effective adsorbate removal. The pore distribution, which may be calculated from the average pore size, results in a reduced BET surface area, as shown in the table. Micropores (less than 2 nm), mesopores (between 2 and 50 nm), and macropores (more than 50 nm) are the three types of pores. Due to high-temperature pyrolysis operations, organic molecules are degraded into volatile gases and liquid tar, and the disposal of tar and volatile compounds to the environment is hastened compared to traditional heating, resulting in activated carbon with a higher carbon content (Hesas et al., 2013).

Table 2.2 Comparison of activated carbon prepared using conventional and microwave heating.

Raw material	Activation technique	Activating agent	Operating conditions	BET surface area (m^2/g)	Average Pore Size (nm)	Adsorption capacity (mg/g)	Ref
Oil palm shell	Conventional	$ZnCl_2$	500 °C; 120 min	1672.00	0.236	N/A	(Hesas *et al.*, 2013)
	Microwave		1050 W; 15 min	1195.00	0.217	N/A	
Bagasse	Conventional	$HNO_3 + H_2SO_4$	500 °C; 90 min	609.00	3.840	12.00	(Wan and Li, 2018)
	Microwave		900 W; 22 min	61.00	8.890	16.00	
Olive stones	Conventional	KOH	715 °C; 120 min	886.72	4.220	17.83	(Alslaibi *et al.*, 2014)
	Microwave		565 W; 7 min	1280.71	4.630	22.73	

2.2.1 Effect of Activation Power

Activation power is just as crucial as activation temperature when it comes to microwave heating. This parameter showed a similar tendency in studies by Foo and Hameed (2012a, 2012b) and Baytar, ahin, and Saka (2018). Foo and Hameed (2012a, 2012b) conducted two tests, one lasting 5 minutes and using a power range of 90 to 800 watts, and the other lasting 30 minutes and using a power range of 200 to 1000 watts.

In Figure 2.1, at a power level less than 180 W, the activated carbon yield and adsorption uptake remained constant, showing no ongoing reaction between the char and activation agent. Whereas from 180 to 800W, a drastic decrease in activated carbon yield was due to the weight loss of carbon. This weight loss of carbon also increased proportional to the microwave power, mainly because of the harsh response at higher thermal radiation which accelerate the devolatilization, dehydration, and decomposition (Foo and Hameed, 2012a, 2012b).

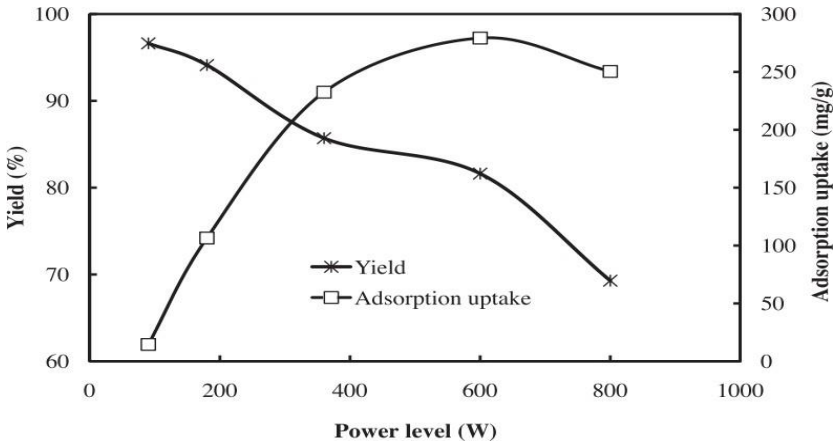

Figure 2.1 Effect of activation power on wood sawdust activated carbon yield and adsorption uptake (Foo and Hameed, 2012b).

At the same time, a drastic increase in adsorption uptake was observed when activation power was increased from 180 to 600W as shown in the Figure 2.1. This

sharp increase in adsorption uptake possibly attributed to the combined effect of internal and volumetric heating which causes the carbon structure to expand and create high porosity and a larger surface area (Foo and Hameed, 2012a). This can be proven the study from Baytar, Şahin and Saka (2018) as shown in Figure 2.2. From 200 to 600W, the surface area of the activated carbon prepared increased from 1088 to 1511m^2/g.

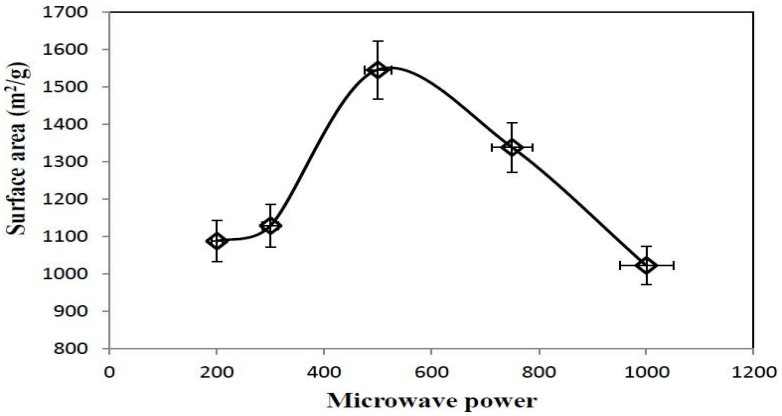

Figure 2.2 Effect of microwave power on sunflower seed husks activated carbon surface area (Baytar, Şahin and Saka, 2018).

Moreover, at radiation power more than 600W, over gasification might occur with the second bread down of the uncompensated gases, which lead to the detrimental effect of reducing surface area and excessive degradation of pore structures (Foo and Hameed, 2012a, 2012b; Baytar, Şahin and Saka, 2018); thus, the adsorption uptake, carbon yield and surface area were progressively decreased.

2.2.2 Effect of Activation Time

Activation time is also another significant factor that will affect the surface area and yield of activated carbon. Based on Shoaib and Al-Swaidan (2015), a longer activation time until an optimum value increased the pore volume and surface area.

Figure 2.3 shows the effect of activation time on the BET surface area, pore volume, and yield percentage of activated carbon. As shown in the figure, when activation time increased from 15 to 30 min, the pore volume and BET surface area of activated carbon increased. At 30 min, the BET surface area (1094m^2/g) and pore volume (0.4382cm^3/g) of activated carbon were the highest with a moderate yield of activated carbon (18.75%).

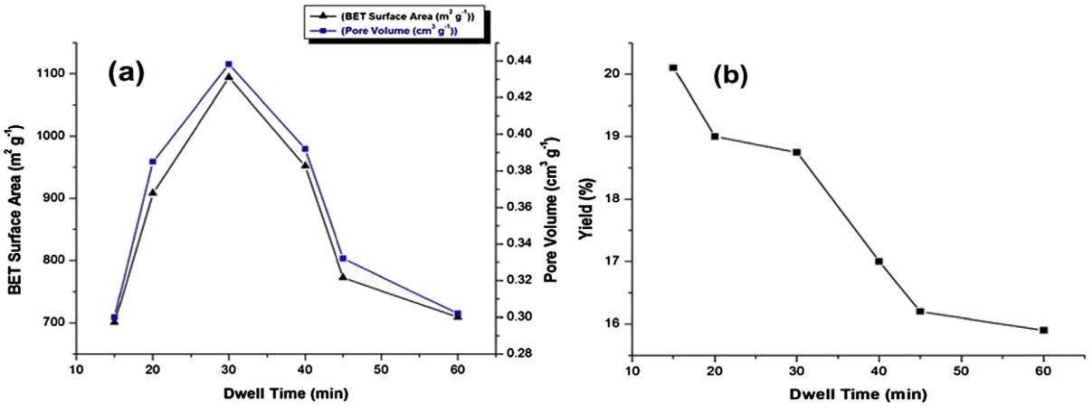

Figure 2.3 Effect of activation time on the BET surface area, pore volume and yield percentage of activated carbon (Shoaib and Al-Swaidan, 2015).

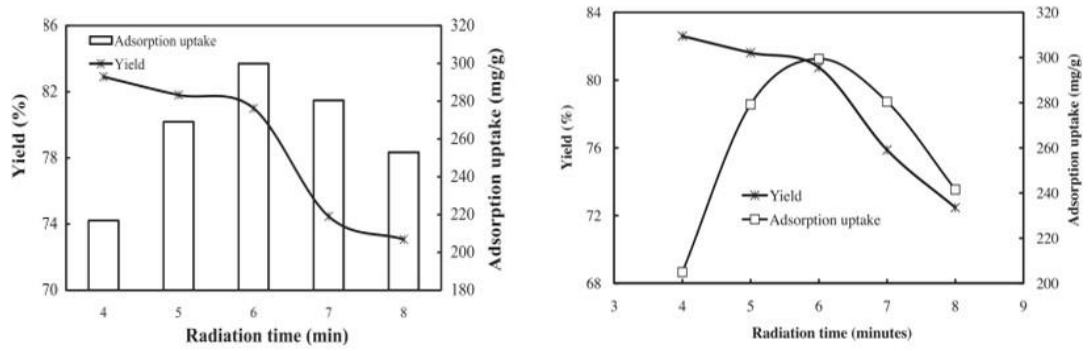

Figure 2.4 Effect of activation time on activated carbon yield and adsorption uptake (Foo and Hameed, 2012a, 2012b).

Similarly, Foo and Hameed (2012a, 2012b) also explored the effect of activation time on the activated carbon yield and adsorption uptake. Both studies revealed similar trend of adsorption uptake and activated carbon yield. When the activation time increased from 2 to 6 min, adsorption uptake increased as well. The

highest adsorption uptake was recorded at 6 min, while the maximum yield percentage was at 4 min. At 6 min, the yield percentage was moderate and comparable. Hence, it is the recommended optimal activation time.

From Figure 2.3 and Figure 2.4, a sharp decline for BET surface area, yield and adsorption uptake was observed when the time was further prolonged. It is most likely due to a sintering effect, which significantly degrades the pore walls between neighboring pores and widens the micropores and mesopores, causing exterior shrinkage and collapse of the carbon framework (Foo and Hameed, 2012b). Furthermore, longer time stimulates the reaction between carbon and activation agents or volatile gas, promoting the breakdown of the C-O-C and C-C bonds and lowering the activated carbon yield (Foo and Hameed, 2012a).

2.2.3 Effect of Activation/ Impregnation Agent

In the study by Foo and Hameed (2012a), activation agents used during the activation has significantly influenced the activated carbon yield and adsorption uptake. By adding an activating agent, pore width was gradually increased and new micropores were produced in the original pore walls, leading to a subsequent increase in BET surface area and pore volume. In the study, H_2SO_4, H_3PO_4, HNO_3, K_2CO_3, NaOH, and KOH were added with the same impregnation ratio of 1:1. Different activation agents gave different activated carbon yield and adsorbate removal at the same operating conditions.

In Figure 2.5, K_2CO_3 gave the highest percentage of activated carbon yield at 85%, whereas KOH resulted in activated carbon that has the highest adsorption uptake at 96 mg/g. H_2SO_4 was considered as the least recommended activation agent since it produces the least activated carbon and lowest adsorption uptake. When sulphuric acid reacts with carbon in char, it introduces oxygen functionalities by the reaction as shown in Eq. 2.1. The key problem is that the water vapour generated will spontaneously deplete the carbon content in the activated carbon as described in Eq. 2.2.

$$2H_2SO_4 + C \rightarrow 2SO_2 + CO_2 + 2H_2O \quad 2.1$$

$$H_2O + C_nH_xO_y \rightarrow H_2 + CO + C_{n-1}H_xO_y \quad 2.2$$

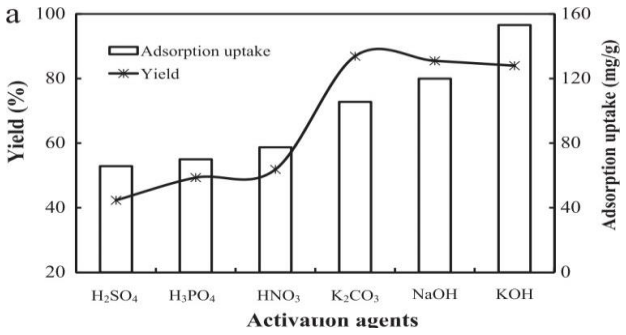

Figure 2.5 Effect of activation agent on activated carbon yield and adsorption uptake (Foo and Hameed, 2012a).

Moreover, K_2CO_3 is a good activation agent to yield the highest activated carbon but the adsorption capacity is moderate. Reduction of K_2CO_3 produces K, K_2O, CO, and CO_2. The potassium compound generated enable to penetrate the interior structure of the char surface, widening the existing pores (Foo and Hameed, 2012b). Next, KOH and NaOH are both alkaline hydroxide activation agents. Porosity is developed through redox reduction and carbon oxidation during alkaline hydroxide activation. Metallic potassium formed during the redox reaction of KOH, similar to that from K_2CO_3, can be intercalated into the matrix independently for separation and

degradation of carbon layers, resulting in the development of the micro and mesopores. In contrast, sodium can only intercalate in highly defective materials. It explains the variation between adsorption uptakes of activated carbons produced using KOH and NaOH, despite their yield percentages being similar. In short, the activated carbon produced using KOH and NaOH as the activation agent is recommended with the high adsorption uptake and comparable yield.

2.2.4 Effect of Impregnation Ratio (IR)

Apart from selecting the best activation agent, the impregnation ratio (IR) also influences the activated carbon characteristics and adsorption efficiency. IR is defined as the dry weight of the activation agent per weight of char as described in Eq. 2.3.

$$IR = \frac{w_{activation\ agent}}{w_{char}} \qquad 2.3$$

Based on the study from Hesas *et al.* (2013), it is concluded that 0.65 is optimal for $ZnCl_2$ to produce palm shell activated carbon using microwave activation. In Table 2.3, raising the IR from 0.15 to 0.65 has gradually increased the S_{BET} of the prepared activated carbon to 1195 m^2/g. The increase of S_{BET} is due to the creation of micropores and mesopores during the activation process. Furthermore, Table 2.3 also illustrates the continuously increasing trend of average pore size and total pore volume with increasing IR. When the IR is increased further to 0.90, the S_{BET} subsequently decreases to 1079 m^2/g. Some of the micropores were slowly being widened and merged into mesopores at higher IR. Excessive activation agent might also degrade or clog some of the micropores. After the optimal amount of activating agent is used for the pore development, the remaining amount of activating agent might form a layer on the pore surface of the activated carbon or block the pores and thus, the diffusion of adsorbate into the interior surface of the activated carbon for adsorption is restricted.

Table 2.3 Effect of IR on surface characteristics of activated carbon (Hesas *et al.*, 2013).

IR	S_{BET} (m^2/g)	Average pore size (nm)	Total pore volume (cm^3/g)
0.15	443	2.04	0.23
0.28	622	2.06	0.32
0.40	738	2.14	0.39
0.53	860	2.15	0.46
0.65	1195	2.17	0.65
0.78	1137	2.26	0.68
0.90	1079	2.43	0.70

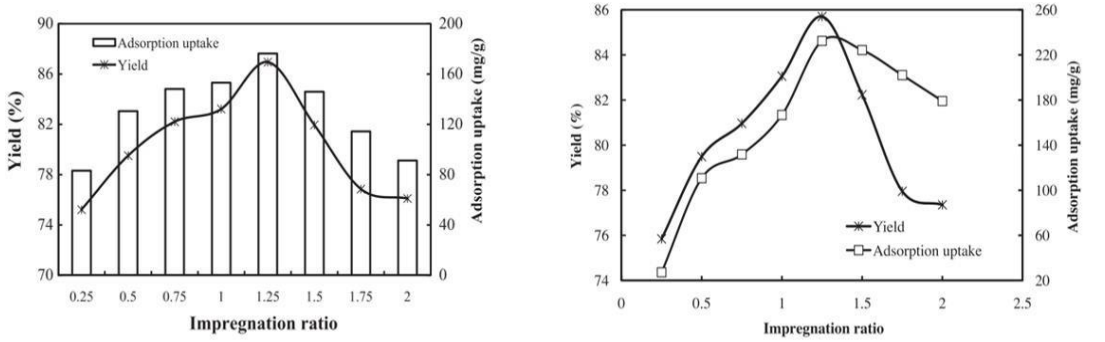

Figure 2.6 Effect of IR (a) KOH (Foo and Hameed, 2012a), (b) K_2CO_3 (Foo and Hameed, 2012b) on activated carbon yield and adsorption uptake.

In 2012, Foo and Hameed (2012a, 2012b) had investigated the IR of KOH to coconut husk and K_2CO_3 to wood sawdust char. According to Figure 2.6, both investigations concluded that 1.25 ratio was the best IR among the range of 0.25 to 2.00 with the highest activated carbon yield (%), and adsorption uptake (mg/g). Beyond 1.25 IR, the subsequent increase in IR reflects a progressive decline in activated carbon yield and adsorption uptake. From the different optimal IR for different agent, a hypothesis can be made: there is no best IR value can be suggested for every impregnation agent.

The drastic decrease in carbon yield and adsorption uptake can be explained by the excessive activation agent such as $ZnCl_2$, KOH, and K_2CO_3 blocks the pores and disrupts the carbon framework in the char. Besides, excessive activation agent like

KOH might decompose to form water vapours which will react with carbon in the char as shown in Eq. 2.4 and 2.5 (Foo and Hameed, 2012a). The vigorous reaction leads to a dramatic decrease of carbon content in activated carbon and reduces the BET surface area.

$$2KOH \rightarrow K_2O + 2H_2O \quad (2.4)$$

$$H_2O + C \rightarrow H_2 + CO \quad (2.5)$$

2.2.5 Mangrove as Raw Materials

Rather than saving money during preparation by applying a better activation condition, as previously discussed, another point of interest is the synthesis of activated carbon from a lost-cost carbon source raw material such as mangrove, which is readily available in Malaysia.

Mangrove stem is abundantly available in brackish water areas in Malaysia. There are 110,953 hectares in Peninsular Malaysia, 139,890 hectares in Sarawak and 378,195 hectares in Sabah as shown in Figure 2.7. The mangrove area available as stated in the figure includes both reserved forest and state land shown in Table 2.4. As from the table, Sabah has the largest mangrove plants area, followed by Sarawak and Perak. Both illustrations show that Malaysia has a total of 629,038 hectares of mangrove plants land available (Omar, Husin and Parlan, 2020). One hectare of mangrove forests can adsorb 42 million tons of carbon in the air or, in other words, the amount of carbon gas emitted from 25 million cars every year. Thus, it is a good carbon source to synthesize activated carbon (Hamid, 2008).

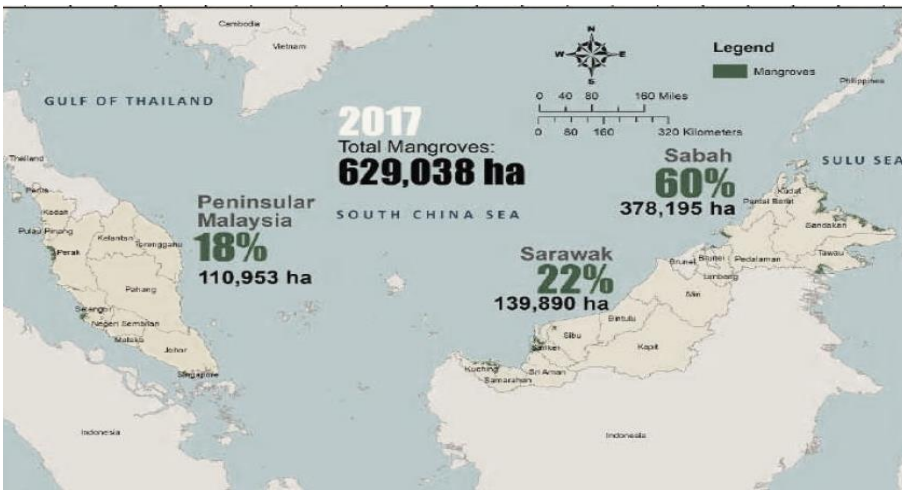

Figure 2.7 Area where mangrove forest can be found in Malaysia in 2017 (Omar, et al., 2020).

Table 2.4 Amount of mangrove forest available in each state of Malaysia in 2017 (Omar, et al., 2020).

State	Total (Hectare)
Perlis	49
Kedah	7725
Penang	1967
Perak	44,990
Selangor	20,853
Negeri Sembilan	1557
Melaka	1241
Johor	26,818
Pahang	3759
Terengganu	1571
Kelantan	422
Sabah	378,195
Sarawak	139,890
TOTAL	**629,038**

2.3 Adsorption Isotherm Model

The pore characteristics related to the activated carbon are obtained from the gas adsorption/desorption isotherm using the Brunauer–Emmett–Teller (BET) method. The six categories of adsorption/desorption isotherms approved by the International

Union of Pure and Applied Chemistry (IUPAC) are depicted in Figure 2.8 (Nishi and Inagaki, 2016).

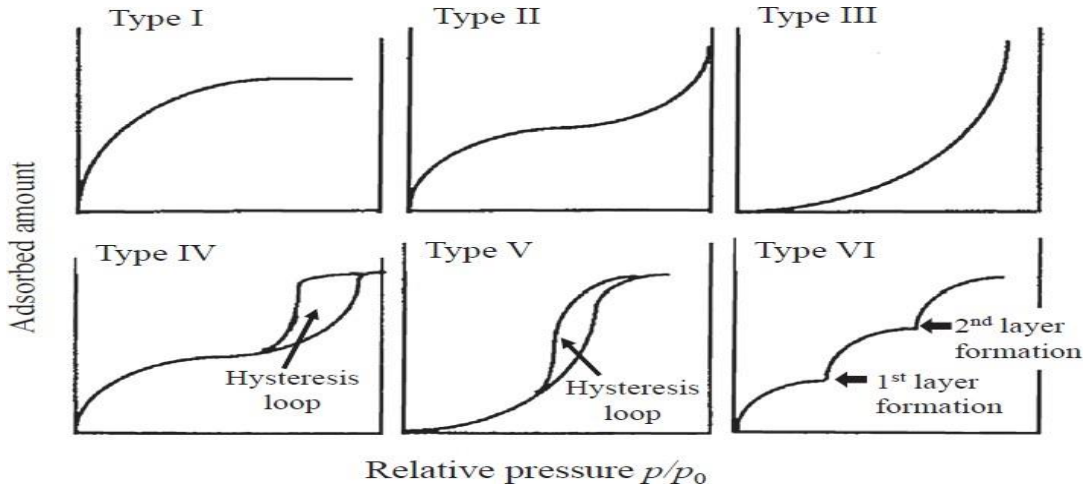

Figure 2.8 Types of isotherms defined by IUPAC (Nishi and Inagaki, 2016).

According to the figure, Type I is a typical microporous isotherm in which adsorption occurs rapidly and significantly up to a relative pressure p/p_0 of 0.1, with the adsorption process reaching equilibrium at p/p_0 of around 0.5. Type II displays monolayer adsorption followed by multilayer adsorption (Nishi and Inagaki, 2016). Type I and Type II isotherms are commonly seen on weak interactive carbon compounds to gas. The isotherm Type III reflects the intermolecular attractive interaction to adsorb gas particles, but without a full surface monolayer like Type IV. The Type IV is a typical isotherm for mesoporous materials that exists between adsorption and desorption curves with substantial hysteresis. Type V is next an extension of Type III, whereby the residual adsorbate condenses in the pore, due to the incomplete monolayer adsorption. Type VI is an adsorption on a highly uniform surface with a gradual isothermal layer-by-layer structure.

Adsorption equilibrium occurs when the concentration of adsorbate adsorbed from the wastewater become constant, and the adsorption isotherm is an interrelationship at this point. The adsorption isotherm is used to estimate various

adsorption parameters, such as maximum adsorption capacity and heterogeneity. Numerous existing adsorption isotherm models can be explored, including Langmuir, Freundlich, Temkin, Hill, Toth, and Redlich-Peterson. Among these isotherm models, Langmuir and Freundlich are the most widely known models applied by Foo and Hameed (2012b, 2012a), Rozaini *et al.* (2010), Salihi *et al.* (2018), Wan and Li (2018) and Wang *et al.* (2011). The correlation of equilibrium analysis is needed for both practical design and a fundamental understanding of adsorption systems.

The appropriateness of the isotherm model is always assessed using correlation coefficient (R^2) as the error analysis. In most cases, the best fit of a graph is chosen based on the comparison of R^2 values to unity (1.0). Nevertheless, in actual practice, the best fit of a graph with R^2 is rarely very close to 1.0 because there is always some degree of mistake caused by the experiment. Thus, it is recommended that a good fit a linear graph with successive R^2 values greater than 0.9 is acceptable. In spite of the fact that the performance of the model is dependent on R^2, it can only be used as a source of reference rather than the primary indicator to determine the biases of the model because when two models have an approximate value of R^2, the model with a lower R^2 might appear to fit better to experiment data after being implemented to non-linear form.

Most of the time, Langmuir isotherm model has a better fit in the linearized equation compared to Freundlich. According to Foo and Hameed (2012b, 2012a), Salihi *et al.* (2018), Wan and Li (2018) and Wang *et al.* (2011), Langmuir isotherm indicates monolayer adsorption whereby the adsorption can occur only at a finite number of localized sites that are identical and equivalent. It also suggests that the adsorption of heavy metal and dye onto activated carbon possesses equal enthalpy and

activation energy as the interaction between the adsorbate particles is neglected, and the energy distribution between the activated carbon is uniform.

On the other hand, experimental data of adsorption of copper (II) ions onto mangrove bark activated carbon in Rozaini *et al.* (2010) is proven to fit the Freundlich isotherm model. It is stated that Freundlich isotherm model describes multilayer adsorption and heterogeneous heat distribution due to the binding sites are not equivalent.

2.4 Adsorption Kinetics Model

The adsorption process is illustrated as a series of stages. The first step is the mass transfer of the fluid phase to the activated carbon particle surface across the external boundary layer film surrounding the outside of the particle. The second step is a rapid adsorption process at individual site on the adsorbent surface and the energy depends on the binding process (physical or chemical adsorption). Lastly, the third step is the diffusion of the adsorbate molecules to an adsorption site either by a pore diffusion process through the liquid-filled pores or by a solid surface diffusion mechanism. Overall, the rate-liming step of the adsorption process will be one or any combination of these steps. Adsorption kinetics models are proposed to determine the potential rate-limiting step. The adsorption kinetics models that were used are pseudo-first-order (PFO), pseudo-second-order (PSO) model, Elovich and intra-particles.

The choice and appropriateness of the kinetics model are always assessed using correlation coefficient (R^2) and normalized standard deviation of adsorption capacity, Δq (%) as the error indicator as shown in Eq. 2.6. From the studies, pseudo-second-order (PSO) kinetics model is found to have a better fit than pseudo-first-order (PFO) for adsorption process (Alslaibi *et al.*, 2014; Aydin *et al.*, 2008; Chen *et al.*,

2011; Foo and Hameed, 2012b, 2012a; Rozaini *et al.*, 2010; Salihi *et al.*, 2018; Wan and Li, 2018; Wang *et al.*, 2011).

$$\Delta q(\%) = \sqrt{\frac{\left(\frac{q_{exp}-q_{cal}}{q_{exp}}\right)^2}{n-1}} \qquad 2.6$$

The best fit of PSO model reveals that the adsorption mechanism is more likely to be the rate-limiting step than the mass transfer of the fluid on activated carbon. Furthermore, PSO also suggests that strong and irreversible bonding (ionic and hydrogen bonding) within the adsorbent surface and adsorbate molecules is involved in the binding action, and the adsorption involves valency forces through electrons sharing between the hydrophilic site of activated carbon and adsorbate cation (Wang *et al.*, 2011; Foo and Hameed, 2012b; Salihi, Kutty and Ismail, 2018). On the other hands, if the kinetic model best fits pseudo-first order kinetic model, the adsorption more favors toward physisorption as the binding action, involving the weak and reversible Van der Waals force within the adsorbent surface and adsorbate molecules (Pourhakkak *et al.*, 2021).

2.5 Factor Affecting The Adsorption Performance

Adsorption performance of an activated carbon is commonly represented by a term called maximum adsorption capacity, Q_{max} which represents the amount of adsorbate adsorbed per unit mass of adsorbent used. Several studies have demonstrated that contact time, initial adsorbate solution concentration, temperature and pH of adsorbate solution and adsorbent dosage are the crucial parameters that will affect the adsorption efficiency of activated carbon (Alslaibi *et al.*, 2014; Aydin *et al.*, 2008; Chen *et al.*, 2011; Foo and Hameed, 2012b, 2012a; Ghaedi *et al.*, 2015; Marda and Astuti, 2017; Rozaini *et al.*, 2010; Salihi *et al.*, 2018; Wan and Li, 2018; Wang *et al.*, 2011).

2.5.1 Effect of Contact time

Based on Alslaibi *et al.* (2014) and Salihi *et al.* (2018), it was agreed that the adsorption is very rapid at the beginning stage. The adsorption capacity and adsorbate removal efficiency increased sharply and the slope of the curve at initial stage is the steepest. This phenomenon was predicted based on the availability of many surface sites for adsorption at the beginning. When times passed, because of the repulsion between the solute molecules of the adsorbate and the bulk phases, the remaining surface sites become more difficult to occupy as the reaction progresses. As equilibrium approaches, the surface sites available was progressively reduced.

Based on Figure 2.9, adsorption of Fe^{2+}, Pb^{2+}, and Cu^{2+} ions onto the olive stone activated carbon studied by Alslaibi *et al.* (2014) is rapid at first 30 mins (0.5 hours) and approaches to constant after 3 hours. The trend also indicates that the effect of contact time on adsorption efficiency is similar for most heavy metal removal. Moreover, Figure 2.10 represents the effect of contact time on Cu^{2+} ions adsorption onto sugarcane bagasse activated carbon from Salihi *et al.* (2018) also suggests a similar trend as in Figure 2.9. The removal efficiency increases sharply during the first 6 hours and slowly reaches an equilibrium after 12 hours. Besides, the different concentration of adsorbate solution with a similar trend indicates that the influence of concentration will not change the effect trend of contact time on the removal efficiency. Figure 2.11 shows the adsorption of Cu^{2+} ions and Ni^{2+} ions onto the modified mangrove bark activated carbon reaches an equilibrium at 60 min (1hour).